Effect of hydroxamate and catecholate siderophores on iron availability in the diatom *Skeletonema costatum*: Implications of siderophore degradation by associated bacteria

N. Sanchez[1], C. K. Peterson[1], Susana V. Gonzalez[1], O. Vadstein[2], Y. Olsen[3], M. V. Ardelan[1]

1. NTNU Norwegian University of Science and Technology, Department of Chemistry, Trondheim 7491, Norway
2. NTNU Norwegian University of Science and Technology, Department of Biotechnology and Food Science, Trondheim 7491, Norway
3. NTNU Norwegian University of Science and Technology, Department of Biology, Trondheim 7491, Norway

Correspondence: Nicolas Sanchez (nicolas.sanchezpuerto@gmail.com)

Key words: Phytoplankton, associated bacteria, organic ligands, siderophores, iron

ABSTRACT

The bioavailability of iron (Fe) across marine ecosystems, mainly determined by Fe speciation and species-specific requirements of phytoplankton, remains largely unresolved. Siderophores are relevant within the pool of organic ligands that control organic Fe speciation. The effect on growth and physiology of the diatom *Skeletonema costatum* following addition over time of the uncomplexed siderophores (apo-form) desferrioxamine B and enterobactin were studied in the laboratory. The diatom was grown in batch culture in concentration gradients up to 50 and 10,000 nM for enterobactin and desferrioxamine B respectively. The potential effect of siderophore degradation was analyzed by electrospray ionization mass spectroscopy (HPLC-ESI-MS). Growth of *S. costatum* was negatively correlated to desferrioxamine concentration. In treatments where more than 500 nM was added, growth was negligible until day 9 after which significant growth started. Fe uptake at day 9 was highest at 10,000 nM, while the Fe quota was the lowest. The addition of enterobactin had a negative effect on the abundance, the *in-vivo* fluorescence and the Fe quota in *S. costatum* only at the highest concentration of 50 nM, while the *in-vivo* fluorescence was enhanced at the lowest concentration. The bacterial abundance over time was also negatively correlated to the concentration for both siderophores, but at day 9 the bacterial uptake showed an increase proportional to the siderophore concentration. HPLC-ESI-MS analysis revealed the presence of tentative metabolites of desferrioxamine in 500 and 10,000 nM indicating changes in concentration of the apo-siderophore. In the presence of

cathecolate and hydroxamate siderophores, *S. costatum* exhibited the capacity for different Fe uptake strategies. The late growth exhibited and the high Fe uptake after prolonged Fe-limited growth, suggests that Fe reduction at cell's membrane may be facilitated by possible degradation of desferrioxamine by the associated bacteria. The results emphasize the need for studying Fe bioavailability of algae together with the interacting bacterial community.

1. INTRODUCTION

At current seawater pH and oxygen content, the thermodynamically stable form of dissolved Fe (DFe) is present at very low concentrations (<0.5 nM) in surface ocean waters (Johnson et al., 1997). More than 99% of DFe is kept soluble by complexation with organic ligands (Gledhill and van den Berg, 1994; Rue and Bruland, 1995). Because Fe is an essential element for growth, marine microorganisms have developed strategies to increase its uptake. For bacteria, production and release of specific iron chelators such as siderophores constitute an adaptive response. These molecules may form part of the pool of organic ligands that solubilize environmental Fe hydroxides and maintain their solubility for biological uptake. From coastal to oceanic ecosystems, several types of siderophores have been isolated and identified for different bacteria (Vraspir and Butler, 2009), and yet there is no complete understanding of the contribution of individual siderophores to the dissolved pool of Fe due to the analytical challenges of detecting low concentrations (Gledhill and Buck, 2012).

While no eukaryotic phytoplankton have been found to excrete siderophores to date, the findings on the use of these organic ligands by marine phytoplankton have been ambiguous (Hopkinson and Morel, 2009). Although substantial advancements has been achieved in the underlying mechanisms (Lis et al., 2015; Shaked and Lis, 2012), there is still a limited understanding of the bioavailability of Fe when complexed by these compounds. For instance, whether the differences in the bioavailability between these compounds have effects on the composition of phytoplankton assemblages or rates of primary production across marine ecosystems (Kustka et al., 2015). Studies conducted to assess the bioavailability of siderophores to eukaryotes have produced mixed results. Most of these studies involve the use of the fungal siderophore desferrioxamine B, of which several have showed negative effects on bioavailability (Eldridge et al., 2007; Eldridge et al., 2004; Hassler et al., 2011; Hutchins et al., 1999a; McKay et al., 2005; Wells et al., 1994; Wilhelm et al., 2013). However, other studies have revealed that eukaryotes have generally low but variable uptake capacities for different Fe-siderophore complexes (Hutchins et al., 1999b). Further studies

have suggested that some eukaryotic phytoplankton can acquire Fe from siderophore complexes through reduction on the cell surface followed by uptake. Among those siderophores are desferrioxamine B (Kustka et al., 2005; Maldonado et al., 2001; Shaked et al., 2005; Strzepek et al., 2011), ferrioxamine E (Maldonado and Price, 1999; Soria-Dengg and Horstmann, 1995), enterobactin and aerobactin (Kustka et al., 2015; Maldonado and Price, 1999; Strzepek et al., 2011).

Most studies suggest that eukaryotic phytoplankton from high nutrient and low chlorophyll (HNLC) waters appear to be more adept at acquiring Fe bound by siderophores than most coastal species, as the result of selective pressures induced by Fe scarcity. Consequently, there has been much less focus on species of coastal phytoplankton such as *Skeletonema costatum* (Hutchins et al., 1999b) or *Phaeodactylum tricornutum* (Soria-Dengg and Horstmann, 1995; Soria-Dengg et al., 2001). Nonetheless, Fe may likely have an equally important regulatory role in coastal waters (Bruland et al., 2001; Hutchins et al., 1998; Öztürk and Bizsel, 2003). Fe requirements of neritic phytoplankton are not only relatively high, but also differ substantially among species. Therefore Fe fluctuations within metal-replete systems could strongly influence the composition and distribution of phytoplankton assemblages (Wells, 1999). At the same time, the coastal environment presents a more complex system because of the input of organic matter, its constituents and their role in the complexation of metals (Breitbarth et al., 2010; Laglera and van den Berg, 2009).

Even though siderophores are believed to be more abundant and more relevant in oceanic environments, the presence of hydroxymate type siderophores has been reported for coastal waters as well (Boiteau et al., 2016; Mawji et al., 2008; Velasquez et al., 2011), suggesting the potentially relevant role of these types of ligands in the costal environment. Furthermore, little effort has been made to study how siderophores are mineralized and recycled via the carbon and nitrogen cycles (Pierwola et al., 2004). In bacteria the Fe(III) uptake occurs via the non-reductive uptake or via the siderophore mediated uptake, where Fe is transported as the Fe(III)–siderophore complex that enters the periplasmic space of gram-negative bacteria through specific outer-membrane receptors (Braun et al., 1998). On the other hand, there is overall little evidence for direct internalization of siderophores by either eukaryotic or prokaryotic phytoplankton (Hopkinson and Morel, 2009). However, More recent evidence though, has shown the use of the non-reductive uptake path for eukaryotic phytoplankton through direct siderophore internalization (Kazamia et al., 2018). While this finding broadens the perspective of different possible metabolic pathways for these organic ligands in

eukaryotic phytoplankton, the end fate for these molecules when internalization does not take place and the siderophore is released back into the environment is less clear. For instance for the α-hydroxyl-carboxylic type siderophores, the photolability of these Fe-complexes results in partial breakdown and changes in the Fe speciation, which may ultimately enhance their bioavailability (Amin et al., 2009; Barbeau et al., 2001; Butler and Theisen, 2010). Although hydroxamate siderophores such as deferrioxamine have been found in seawater and are excreted by a species of marine bacteria (McCormack et al., 2003, Gledhill 2004), the fate and possible role of siderophore breakdown products is less known.

High-Performance Liquid Chromatography with Electrospray Ionization Mass Spectrometry (HPLC-ESI-MS) has been employed as a tool for identifying siderophores in the marine environment matrix (Gledhill, 2001; Gledhill et al., 2004; Mawji et al., 2008; McCormack et al., 2003). Different to chemical assays such as CAS or Rioux (Haygood et al., 1993; Martinez et al., 2001), the use of HPLC-ESI-MS allows for detection of the metabolites and byproducts of siderophores (Pierwola et al., 2004; Winkelmann et al., 1999). Here we combined the use of culture experiments together with HPLC-ESI-MS analysis to determine the presence and the effect of different types of siderophore on the Fe bioavailability for one phytoplankton species from the coastal environment. We conducted a batch culture with *Skeletonema costatum* with semi-continuous addition of apo- siderophores desferrioxamine B and enterobactin in a concentration gradient. The Fe uptake and Fe quota were measured to compare adaptation strategies with different siderophores as a function of time. The detection and role of siderophore metabolites is discussed based on the role of the species-specific interactions between phytoplankton and the associated bacteria present in the culture.

2. MATERIALS AND METHODS

2.1 Water collection and conditioning

Water collected for the cultures was obtained from the seawater intake at the laboratory facilities of the Trondheim Biological Station (63°N) at NTNU, Trondheim Norway. The water intake is located at a depth of ~80 m with a bottom depth of ~100 m. Water was collected during November 2015, when concentrations of total dissolvable Fe in the Trondheim fjord (10 - 50 m) have been found to range from 5 to 12 nM (Öztürk et al., 2002). A volume of 150 liters was collected in acid-washed 20 L polyethylene (PE) Nalgene bottles. All water was filtered through acid washed filters (0.45 + 0.2 μm Sartorius Sartobran 300).

To condition the seawater to low iron concentrations, an ion exchange resin (Chelex-100 - Bio-Rad Laboratories) was used to complex most kinetically labile forms. 2 ml of Chelex-100 slurry (~0.4 gr dry weight) was added to each 10 L bottle of water and placed on a shaker for 24 h at room temperature. Afterwards, the seawater was filtered through a silicon tubing using a peristaltic pump, passing all content through an acid-washed poly-prep chromatography column with a built-in polyethylene frit (pore size 100– 300 µm size; Bio-Rad Laboratories) with an extra 0.5 ml Chelex-100 slurry at a rate of 3 mL min^{-1}.

To determine the background Fe concentration, triplicate samples were collected, pre-concentrated and extracted using a batch (Baffi and Cardinale, 1990) and column technique (Ardelan et al., 2010). To each 150 ml water sample, 0.2 ml of ion exchange resin Toyopearl AF-Chelate 650 M (Tosoh), was added and then placed for 12 h on a shaker (~80 rpm). The extraction of trace elements proceeded using a chromatography column (see above), and in a 2-step acidifying process first by adding 1M UP HNO_3 and then by 0,25M UP HNO_3 for a final 3 ml sample. Initial background concentrations of DFe labile were 1.22 ± 0.3 nM, while the total dissolved Fe concentration (TDFe) was 2.59 ± 0.46 nM. The former fraction corresponds to the Fe complexed by the resin at seawater pH, while the latter corresponds to the Fe fraction complexed after acidification (pH~1.7) of the sample for about months after bringing back the pH to ~6 for extraction. All samples collected to determine DFe as well as the manipulation of the experimental bottles during addition and sampling were performed in a Class-100 laminar flow hood (AirClean-600 PCR Workstation) which minimized possible contamination. The analysis was performed by High Resolution Inductive Coupled Plasma Mass Spectrometry (HR-ICP-MS) Element 2 (Thermo-Finnigan) with PFA-Schott type spray chamber and nebulizer.

2.2 Culture setup

The experiments were conducted in a temperature-controlled room (14.5 to 15.0 °C) at 40-60% humidity. The light regime was a 24 h light cycle with fluorescent lighting and a mean luminous intensity of 80 – 90 µmol $m^{-2}s^{-1}$. The species used in this study was *Skeletonema costatum* (NIVA-BAC 36 strain culture-CAA) provided by the Norsk Institutt for vannforskning (NIVA). The strain was maintained in a normal f/2 medium (Guillard and Ryther, 1962) and was transferred to low Fe media for the experiments. The cultures were grown in an EDTA/metal ion buffered seawater medium modified from the artificial algal culture medium Aquil (Price et al., 1989). All macronutrients (Nitrogen, Phosphorus and

Silicon) were prepared and kept as independent stock solutions that were passed through a column containing Chelex-100 to remove Fe. Trace metal enrichment was based on a doubled concentration of EDTA (10 μM) of the original Aquil, adjusting the total concentration of each metal to achieve the same free ion concentration for pCu (13.79), pMn (8.27), pZn (10.88) and pCo (10.88). Fe was added as part of a mixed trace metal solution + EDTA at a concentration corresponding to a pFe of 18.2 in order to guarantee sustained growth for the duration of the experiment.

The species used in this study was *Skeletonema costatum* (NIVA-BAC 36 strain culture-CAA) provided by the Norsk Institutt for vannforskning (NIVA). The strain was maintained in a normal f/2 medium (Guillard and Ryther, 1962). The inoculum added to the experiment was from at least the second batch culture run in a low Fe growth medium in order to adapt the species to low Fe concentrations and to minimize all possible Fe transfer from the original f/2 medium. The original culture strain of *S. costatum* was non-axenic and bacterial abundance was quantified by flow cytometry (see section 2.4).

2.3 Experimental setup and sample collection

Thirty-six 500 mL acid-washed polycarbonate (PC) bottles were used in total, where each treatment involved three bottles (triplicates). Before the algae inoculation, all bottles contained the Aquil media and all macro- and micro-nutrients required in the culture. Half of the bottles (18) were used for the setup with the siderophore desferrioxamine while the other half were used with the siderophore enterobactin. For the treatments established with each siderophore, see section 2.8.

Every third day a 10 mL sample was collected from each one of the thirty-six bottle for measuring pH, photosynthetic efficiency (F_v/F_m), *in-vivo* fluorescence (FSU), cell densities of algae and bacterial densities. At the end of the experiment, samples for DFe were collected using Toyopearl resin (see above). To estimate the photosynthetic efficiency, an aliquot of the subsamples was placed in a cuvette (under dim light) and measured on a field portable device AquaPen-C 100 (Photon systems instruments). A Turner designs (Trilogy) fluorometer was used for FSU measurements. The growth rate, estimated in doublings per day (d^{-1}), was calculated from the linear regression of the Ln FSU *versus* time (Guillard, 1973). The initial algal cell density for both cultures was ~8000 cells mL^{-1}.

2.4 Bacterial abundance

At start, middle and end of the experiment samples (1.5 mL) were fixed with Glutaraldehyde (final concentration 1 %), frozen in liquid nitrogen and then stored (-20 ºC) until analysis by flow cytometry (Marie et al., 1997). Samples were diluted 1:10 or 1:100 with 0.1x TE-buffer, depending on cell density. The DNA of bacterial cells was stained with 10 µL 1:50 diluted SYBR Green I Nucleic Acid Gel Stain (10.000X in DMSO; Molecular Probes) per 1 mL diluted sample, and incubated in the dark (15 m) before analysis. Flow cytometry analysis were performed on a BD Accuri C6 Flow Cytometer (BD Bioscience, San Jose) and blue laser (excitation 488 nm). All samples were analyzed with the same instrumental setting: medium flow rate (34.5 µL min^{-1}), FL1 threshold of 2000 and sample collection for 3 min. Medium flow rate was used for highest accuracy when counting bacterial cells.

2.5 Fe uptake

Fe radioisotope short-term uptake measurements were performed for selected treatments (Table 2) at day 9 (corresponding to the end of exponential phase in the Control). For each selected treatment, triplicate PC bottles were spiked with Fe-55 as ferric chloride in 0.5 M HCl (2 mCi, specific activity on the day of experiment of 42.22 mCi/mg; Perkin Elmer). 0.030 mL of ferric chloride were added from a Sub-stock (0.7 mCi), in order to reach final concentration of ~0.5 nM. Bottles were incubated in lighted conditions for 16 h, after which filtration was performed sequentially with 10 µm and 0.2 µm PC filters. Each filter was individually washed with oxalate reagent for a 10 – 15 min period to remove extracellular Fe (Hassler and Schoemann, 2009; Tovar-Sanchez et al., 2003). The solvent extraction step from Tovar-Sanchez et al. (2003) was omitted and Chelex-cleaned seawater was used for rinsing instead (Tang and Morel, 2006). Fe uptake was calculated for both fractions using the liquid scintillation counts (corrected for filter quenching) and DFe concentrations in the cultures (Schmidt and Hutchins, 1999). Measurements of particulate organic carbon (POC) were used for normalizing uptake rates of Fe:C (µmol:mol h^{-1}) in the >10 µm fraction. For the >0.2 µm fraction, the Carbon content was estimated based on the bacterial abundance at day 9 and applying a carbon content factor of 30.2 ± 12.3 fg of C $cell^{-1}$ (Fukuda et al., 1998). Uptake rates were also standardized by cell area according to a cylinder area estimation (Sun and Liu, 2003) based on microscope measurements for at least 100 diatom cells (Table 2).

2.6 Particulate Fe (PFe) and Fe quota (FeQ)

PFe was determined by low-pressure (< 0.5 bar) vacuum filtration through 10 μm acid washed 47 mm polycarbonate (PC) filters. Filtration volume ranged from 100 to 1000 mL for large replicates (see below) depending on cell density. Each filtration was followed by oxalate rinsing of the filter (see above), and samples were kept frozen until further processing. Samples underwent High Performance Microwave Reactor (Ultra Clave UC Milestone) digestion by placing the filters into Teflon tubes, adding 5 mL of 7 M ultra-pure HNO_3, then placing the filters inside the UC for two hours. After digestion, the samples were diluted with deionized water (18.2 MΩ) to reach a final sample concentration ~0.6 M HNO_3 for HR-ICP-MS analysis. Particulate organic phosphorus (PP) obtained in each fraction was used for the normalization of the PFe and to calculate of the Fe:P ratio (mmol:mol).

2.7 Statistical analysis

Data analysis for the physiological and biological parameters measured was performed through parametric tests after homoscedasticity was determined. For analysis between different treatments, analysis of variance (one-way ANOVA) and Tuckey HSD Test for differences were performed. For 2-way comparisons between siderophores at the same concentration, Student-t tests were performed. All significant differences referred throughout the results were set to a level of 0.05.

2.8 Siderophores characteristics and experimental additions

Desferrioxamine B (DFB-Sigma) is a hexadentate ligand with hydroxamate functionalities and linear acyclic architecture (Albrecht-Gary et al., 1998). It is a strong Fe-complexing agent, with a conditional stability constant of $10^{16.5}$ M with respect to total inorganic Fe (Fe′) in seawater (Hudson et al., 1992). Enterobactin (Sigma) is also a hexadentate ligand belonging to the catecholate siderophores and is characterized by extremely high stability constants for Fe, up to 10 orders of magnitude higher than hydroxamate siderophores (Granger and Price, 1999; Reid et al., 1993). Both DFB and enterobactin form photostable complexes (Barbeau et al., 2003; Finden et al., 1984; Raymond et al., 2003). Despite the higher stability constant with respect to ferric ion of enterobactin, it has been regarded as a Fe-complex which is readily bioavailable for some eukaryotic phytoplankton (Hutchins et al., 1999b; Strzepek et al., 2011).

Based on the different chemical properties of DFB and enterobactin, two different (but comparable within a specific range) concentration ranges were employed. DFB which exhibits a lower stability constant and a lower capacity to solubilize Fe compared to enterobactin (Boukhalfa and Crumbliss, 2002), was used on an ample concentration range. The concentration gradient used with DFB reached the micro molar level, in order to ensure complexation of all Fe available, while also having siderophore in excess to determine the concentration at which algal growth would not be possible. The gradient employed with enterobactin, was also high enough (50 nM) to achieve full Fe complexation but given the high bioavailability attributed to enterobactin, a lower concentration range was used to observe for potential positive effects on the physiological traits of the diatom. Accordingly, the lower range in DFB additions were comparable to the higher range with enterobactin.

To set each siderophore gradient (treatments), five discrete siderophore additions, plus one control were established (Table 1). Different to all macro- and micro-nutrients additions, the siderophore additions were performed in a semi-continuous way (partial additions) throughout the experiment (at the beginning and every third day for five days) after sample collection until achieving the final target concentrations (day 11). The semi-continuous addition of the uncomplexed siderophore (apo-form) intended to 1.) recreate the natural process when siderophores are released in the environment, thus achieving a rather constant Fe supply with the apo-siderophore that allows competition against the pool of organic ligands already present and 2.) study the adaptive responses from the diatom at different starting concentrations, together with incremental additions of the siderophore over time.

2.9 Solid phase extraction and HPLC-ESI-MS of dissolved organic matter

For selected DFB and enterobactin additions, large volume (5000 mL) batch cultures (duplicates) were run in parallel using sixteen low-density polyethylene (LDPE) collapsible bottles in exactly the same way and time as the low volume cultures. Additionally, for each siderophore, one “No-Algae” treatment were run in duplicates (Table 3). The latter contained only seawater medium, plus a siderophore addition and was used as an abiotic control for potential effects of temperature and light on the siderophores.

Solid phase extraction (SPE) of the dissolved organic matter was carried out following the procedure from Dittmar et al. (2008). Samples were filtered (0.2 µm Whatman pre-combusted GF/F filters) and acidified (HCl 32%) to ~pH 2. SPE cartridges (Agilent Bond Elut PPL, 500 mg 6 ml) retain molecules with a wide range of polarity. The cartridges were rinsed with

methanol (5 ml) before running the samples through. Salts were removed with HCl (10 ml ~0.01 M) and of the dissolved organic matter was eluted into glass vials with ~8 ml of methanol (HPLC grade sigma). Samples were stored at -20 °C until analysis.

To detect possible changes in the relative abundances of the siderophores over time, together with the possible presence of siderophores metabolites in the different treatments, a non-targeted LC-MS^E (MS/MS) analysis were performed on a Waters™ Acquity uHPLC Synapt-G2S Q-TOF system using ESI in positive mode. A Waters™ HSS T3 100 mm column was used for separation with two mobile phases, A: Water (w/ 0.1 % formic acid) and B: Acetonitrile (w/ 0.1 % formic acid). The ESI source used a capillary voltage of 3kV. Leucine enkephalin (1 ng ml^{-1} with a flow of 10 µL per min) was used for lock mass correction With a run time of 13.50 min, the LC gradient was initially at 94% A and 6% B, after 9 min at 60% A and 40% B, after 12 min at 0% A and 100% B and finally after 13 min at 94% A and 6% B, with a flow rate of 0.300 ml min^{-1}. MassLynx v4.1 was used for instrument handling.

2.10 Identification of siderophores and siderophore metabolites

From each SPE sample obtained, three subsamples (pseudo-replicates) were obtained making a total of two samples and six subsamples per treatment for HPLC-ESI-MS. Data processing and analysis of LC-MS data was performed with the software Progenesis QI v2.2. The non-targeted approach allows to carry out a semi-quantitative analysis of known and unknown compounds present in the treatments. The data for the compound ions within the different treatments was normalized in a standard procedure of software Progenesis QI, to correct for possible technical variation between sample runs. The normalization was followed by standardization to show the relative standard deviation from the mean for each compound among treatments. The standardized normalized abundance is hereafter referred to as abundance. Following the normalization for all data, a between-subject experimental design (assumed independence between treatments), and principal component analysis (PCA) were used to determine potential correlations for compound ion abundances found for each treatment. Previous comparisons were made with seawater blanks with the same seawater.

The available literature was used for identification of DFB (Velasquez et al., 2011), enterobactin (Berner et al., 1991) and its tentative metabolites (Groenewold et al., 2004; Pierwola et al., 2004; Winkelmann et al., 1999). The abundance for the apo- and Fe-siderophores and tentative metabolites that showed significant differences ($P < 0.05$) were selected and matched with databases (Chemspider, Progenesis Metascope, and Metlin).

3. RESULTS

3.1 *Skeletonema costatum* response under DFB and enterobactin

Figure 1 shows the trend over time for the variables measured every third day on the diatom culture upon addition of the siderophores DFB (left panel) and enterobactin (right panel). The growth pattern over time exhibited by *S. costatum* with added DFB was negatively correlated to the siderophore concentration. The treatments with low DFB concentrations exhibited a shorter lag-phase similar to that in the Control while higher DFB additions resulted in a delayed growth response.

The general pattern over time in the Control showed peak abundance at day 9, reflected in maximum FSU, with a consistent response in the other variables measured. For comparison, the 500 and 10,000 DFB nM treatments presented respectively ~50 and 10 % of FSU in the Control (Fig. 1c). Despite the longer lag-phase for higher DFB treatments, final cell biomass in these treatments reached similar (~80 % on average) levels to those achieved in the Control. *S. costatum* cultures with added enterobactin showed no general trend as a function of siderophore concentration for the different variables measured, FSU being the only exception. At the lowest enterobactin concentration (0.01 nM), FSU exhibited the only significantly positive effect compared to the Control, while the highest enterobactin treatments (2.5 and 50 nM) exhibited negative trends (Fig. 1d). The negative effect in the FSU at 50 nM was significantly larger for enterobactin than for DFB.

Growth rate during the exponential phase in the 10 to 500 nM DFB treatments showed no significant differences as compared with the Control (1.1 d^{-1}), whereas growth rates in the 2500 nM (0.92 d^{-1}) and 10,000 nM (0.85 d^{-1}) DFB treatments were significantly lower. Growth rates of cultures with added enterobactin showed no significant differences between treatments (Fig. 2).

3.2 Fe uptake and quota in *S. costatum*

On day 9, the difference in cell density between the Control and the highest DFB treatment was at a maximum. The FeQ and Fe uptake for *S. costatum* showed contrasting results between treatments (Fig. 3a). Fe uptake for all treatments with added DFB was significantly higher than the Control (Fe:C, 0.0031 μmol mol h^{-1} or 0.04×10^{-21} mol Fe μm^{-2} h^{-1}), with the 10,000 nM DFB being 1 and 2 orders of magnitude higher on a carbon and cellular area basis respectively (Table 2). FeQ showed the opposite trend with both 500 and 10,000 nM DFB

347 treatments with significantly lower FeQ than Control (Fig. 3a). At the end of the experiment
348 (day 13), *S. costatum* with 500 nM DFB had a FeQ similar to that in the Control. At 10,000
349 nM DFB, despite the increase in cell abundance over time FeQ remained the lowest among
350 treatments. For *S. costatum* cultures with added enterobactin, Fe uptake rates were not
351 significantly different between treatments, although the exhibited trend was the same as for
352 DFB. In the concentration range of enterobactin (up to 50 nM), there were no significant
353 differences in uptake rates between FeDFB and FeEnterobactin (Table 2). The FeQ at 0.01
354 nM was significantly lower than the Control, and remained the lowest throughout the
355 experiment. The FeQ at 50 nM was significantly lower at day 13 compared to day 9 (Fig. 3b).

356 **3.3 Total bacterial abundance and Fe uptake**

357 The effect of DFB on the >0.2 μm fraction containing the bacteria in *S. costatum* cultures was
358 the same as that observed in the diatom (Fig. 4a). At day 9, bacterial abundance was
359 significantly lower at high DFB concentrations. Final bacterial abundances in the Control and
360 10 nM DFB were not significantly different, whereas in the 10,000 nM DFB it was <50% of
361 the Control. In cultures with added enterobactin, the concentration range used had the same
362 effect as DFB, with the highest treatments (2.5 and 50 nM) presenting significantly lower
363 abundances compared to the Control. At the same siderophore concentration (50 nM), no
364 significant differences were found in final bacterial abundances between cultures with added
365 DFB and enterobactin.

366 Fe uptake measured at day 9 presented significant differences between treatments for DFB
367 and between siderophores at comparable concentrations (Fig. 5). In cultures with added DFB,
368 uptake rates in the 10 and 500 nM treatments were less than half of the Control, whereas the
369 uptake rate for the 10,000 nM DFB treatment was significantly higher. In cultures with added
370 enterobactin, Fe uptake was proportional to the siderophore concentration. All uptake rates
371 were higher than in the Control, although only the 50 nM enterobactin treatment was
372 significantly higher than the Control.

373 **3.4 Final labile DFe**

374 Final DFe concentrations in cultures with added DFB presented significant differences
375 between treatments (Table 4). DFe in the Control was just slightly higher than initial
376 background DFe. A gradient was observed in the treatments with the lowest DFe at 10 nM
377 and the highest at 10,000 nM DFB. Only the latter presented a higher final DFe than the

Control, whereas DFe at 10 and 50 nM DFB was significantly lower. In cultures with added enterobactin, a similar trend to the DFB culture was observed. DFe at 0.05 nM enterobactin was significantly lower than the Control, while DFe at 50 nM enterobactin was 3-fold higher than at 50 nM DFB.

3.5 Desferrioxamine, FeDFB and identification of metabolites

DFB was identified by a retention time of 4.30 minutes with an m/z value of 561.3616. Data from collision-induced dissociation (CID) rendered a fragmentation spectrum that matched that in the literature (Supplement-Fig. 1). Ferrioxamine was found at 2.95 min with 614.2710 m/z. No fragmentation data was obtained for this compound, but Fe presence was confirmed by the ^{54}Fe, ^{56}Fe isotopic pattern (Supplement-Fig. 2). Figure 6 shows abundance profiles for DFB and FeDFB for each one of the treatments.

The distribution of DFB and all compounds present in the HPLC-ESI-MS data showed clusters according to the different siderophore treatments (Fig. 7). The 1st principal component (PC1) accounted for ~ 60% of variance and separated the highest DFB treatment and the No-Algae 500 nM DFB treatment from the two lowest DFB treatments. This arguably reflects the abundance of metabolites in each treatment produced by *S. costatum* during biomass growth. This was reflected in the 500 nM DFB and No-Algae 500 nM DFB treatments, which despite having the same DFB concentration were negatively correlated. PC2 accounted for ~25% of the variance, and separated the10 nM from the 500 nM DFB treatments. The apo-siderophore presence was positively correlated to the 10,000 and No-Algae 500 nM DFB treatments, while negatively correlated to lower DFB. Ferrioxamine showed the opposite trend, positively correlated to lower DFB concentration.

Additional to the identification of DFB and Ferrioxamine, three other compounds ions from the LC-MS data identified as tentative metabolites of DFB, showed significant differences between treatments (Table 5). A dihydroxamate compound ion with 419.2503 m/z eluted at 3.41 min and matched the chemical formula. According to the PCA it was most abundant in 500 nM DFB (Fig. 8a), but the loadings indicated no DFB correlation. A monohydroxamate (319.2348 m/z) eluted at 4.26 min (Fig 8b), showing highest abundance in 10,000 nM DFB and was found close to DFB on the scores plot (Supplement- Fig. 3). At 4.31 min, another monohydroxamate (201.1240 m/z) also eluted. It had the same suggested chemical formula and highest abundance in 500 nM DFB, but was also present in 10,000 nM DFB. The loadings showed no strong correlation with DFB (Supplement-Fig. 4).

3.6 Enterobactin relative concentration

The apo-siderophore with a 670.1525 m/z, eluted at 9.81 min towards the end of the time window indicating the hydrophobic nature of the molecule. The compound's identity was confirmed by its fragmentation data with the primary fragment 224 m/z being 1/3 of the original molecule (Supplement-Fig. 5). No fragment representing the other 2/3 of the molecule at 447 m/z was identified. Figure 9 shows abundance profiles for enterobactin for each one of the treatments. The Fe-Enterobactin complex was not detected in any treatment. Although the low concentrations additions of the apo-siderophore were detected in all treatments, the PCA showed that the sample replicates did not cluster properly by treatments (Fig. 10). This was observed in the low replicability in the 50 nM and No-Algae 50 nM treatments. The lowest (0.01 nM) enterobactin treatment exhibited the highest similarity between replicates and pseudo-replicates. The PCA showed overlap of treatments, indicating no significant differences (Supplement-Fig. 6). The PC1 accounted for 56% of the variance and negatively correlated the algae with the No-Algae treatments, indicating that metabolites (products of biomass increase) were the main components of the variation. The PC2 accounted for 22% of variance, however no trend with the enterobactin concentration was observed. The overlap in treatments may be the result of the similar biomasses attained.

4. DISCUSSION

Most of the research conducted on Fe bioavailability in diatoms has been based on the genus *Thalassiosira* and therefore there is still limited information for comparisons with species from other genera. The diatom *S. costatum* has been previously studied under the presence of other organic ligands, involving only hydroxamate type siderophores (Hutchins et al., 1999b; Sanchez et al., 2018). For *S. costatum*, the growth pattern and siderophore response observed was consistent with previous experiments conducted under similar conditions with only DFB (Sanchez et al., 2018).

4.1 Siderophore type and supply rate and in the culture

The kinetics of Fe exchange between competing ligands suggest that the reaction in hydroxamate siderophores such as DFB may require longer to reach equilibrium compared to catecholate siderophores such as enterobactin. Instead of providing the already pre-complexed Fe, through the semi-continuous supply of the apo-siderophore over time it could be allowed for these two types of siderophores to reach the equilibrium with the others

ligands present in natural seawater. The results obtained with both siderophores argue for the relevance of the approach with a rather continuous supply of the apo-form of the siderophore. Compared to short-term Fe uptake experiments (Maldonado et al., 2001; Maldonado and Price, 1999) under exponential growth with already pre-complexed Fe as the only source, the approach applied here can account for the adaptation of the algae over a wider time window. This can ultimately offer a different perspective on the Fe uptake in the algae.

4.2 Fe uptake and response of *S. costatum* with FeDFB

Fe uptake measured at day 9 corresponded with the largest differences observed among treatments, as was evident in variables such as pH and FSU. Accordingly, the highest uptake at 10,000 nM DFB and the lowest in Control likely reflected the physiological state and therefore the different growth phase of *S. costatum* in each treatment. Fe uptake rates in the Control ($0.04x10^{-21}$ mol Feμm^{-2}h^{-1}) and 50 nM DFB ($0.07x10^{-21}$ mol Feμm^{-2}h^{-1}) were in the range measured for "Fe-sufficient" cells for the diatom *T. oceanica* (Maldonado et al., 2001). On the other hand, the Fe uptake rate at 10,000 nM DFB ($1.25x10^{-21}$ mol Fe μm^{-2}h^{-1}) resembled more "Fe-limited" cells (Maldonado and Price, 2001). Results here arguably reflect the Fe uptake dependence on up-regulation in the number of cell surface Fe-transport systems (Hudson and Morel, 1990), that can occur both under varying Fe-siderophore complex (Maldonado and Price, 2001, Strzepek et al., 2011) or apo-siderophore concentrations (Sanchez et al., 2018).

The two main approaches to assess uptake rates can be summarized by 1) one in which increases of FeDFB alter the total Fe concentration (Maldonado et al., 2001; Strzepek et al., 2011), and 2) one in which either Fe or DFB concentrations vary to alter the Fe′ (Maldonado et al., 2000). Most observations suggest diatoms respond more positively to the former. In this study, we varied the DFB concentration in order to alter Fe′. Accordingly, the growth rate in *S. costatum* responded to a decreasing Fe′ with increasing apo-siderophore concentration, resulting in increased Fe uptake mediated by up-regulation of cell surface Fe-transport systems. However, based on reduction half-constant estimations for the FeDFB complex (Nodwell and Price, 2001) the high DFB to Fe ratios applied here would have constrained Fe uptake in the algae if it were solely dependent on the Fe-complex reduction rate. Furthermore, Fe uptake at 10,000 DFB nM was ~8-fold higher than in Maldonado and Price (2001) at similar [DFB]:[Fe] ratios. In cultures with oceanic species of *Thalassiosira,* reduced Fe uptake rates caused ~ 40% growth decrease at a [DFB]:[Fe] > 400, whereas in the

coastal species *T. pseudomona* and *T. weisflogii*, no growth occurred at the same [DFB]:[Fe] ratio (Strzepek et al., 2011). Similar studies in coastal phytoplankton reported that addition of DFB eliminated Fe uptake by both phytoplankton and heterotrophic bacteria, with only marginal Fe uptake after 5 days (Wells, 1999). Nonetheless, studies in coastal diatoms have also reported the acquisition of organically complexed Fe, such as FeDFB in *P. tricornutum* (Soria-Dengg and Horstmann, 1995), *T. pseudomona* and *T. weissflogii* (Shaked et al., 2005). Despite the different responses between species and concentrations of siderophore, most evidence indicate that coastal phytoplankton is more susceptible to organically complexed Fe, therefore highlighting the response observed in this study.

On the other hand, differences in FeQ observed along time point to the degree of physiological adaptation of the diatom, suggesting that depending on the siderophore concentration some of the effects were rather temporal than permanent features. This could be observed at 500 nM DFB, when at day 9 FeQ in *S. costatum* was lower than the Control but by day 13, it had reached similar values. Conversely at 10,000 nM DFB, despite increased Fe uptake and cell density, by day 13 the FeQ in the algae remained the lowest. The effect of DFB on FeQ in other diatom species has been previously reported to have significant reductions at higher siderophore concentrations (Strzepek et al., 2011).

4.3 Fe uptake and response of *S. costatum* with FeEnterobactin

Although regarded as highly bioavailable compared to other Fe-siderophore complexes, the literature on FeEnterobactin uptake in marine phytoplankton is also scarce and shows different responses among species (Hutchins et al., 1999b; Kustka et al., 2015; Strzepek et al., 2011). In *T. oceanica* cultures under 4:400 [Fe]:[enterobactin] a 50% growth yield with respect to Fe′ was observed. On the other hand, the coastal species *T. pseudomona* and *T. weissflogii* did not grow even at a 4:40 [Fe]:[enterobactin] ratio (Strzepek et al., 2011). In *S. costatum*, reported uptake rates range from ~0.19 μmol mol h^{-1} Fe:C under Fe′, to ~0.07 and 0.02 μmol mol h^{-1} respectively with protoporphyrin and ferrichrome complexes on a 1:5 ratio (Hutchins et al., 1999b). At a similar FeEnterobactin ratio (~1:1.2) to that used here, Fe uptake was 0.01± 0.005 μmol mol h^{-1}, similar to that for ferrichrome.

In contrast to the algae response to FeDFB, enterobactin seemed to exert both a positive and negative response on variables such as FSU and abundance which was dependent on the siderophore concentration. The increased FSU at lower FeEnterobactin, contrasted with the observed FeQ, which remained the lowest throughout. Moreover, FeQ in the Control and 50

505 nM treatments did not differ significantly on day 9, but this changed by day 13 with a ~35%
506 decrease at 50 nM. This suggests a significant impact over time of enterobactin compared to
507 DFB at the same concentration. On the other hand, Fv/Fm, pH and the estimated growth rate
508 did not show significant differences. The irregular effect on the overall variable responses has
509 also been reported for growth and Chl-a yields under a 0.5:1 [Fe]:[enterobactin] ratio, where
510 a ~ 2 fold increase in growth respect to the Control contrasted with a Chl-a yield of ~60% of
511 the one achieved in the Control (Kustka et al., 2015). Nonetheless, judging by the growth rate
512 and final abundances reached the effects of FeEnterobactin might have been only temporal.
513 Furthermore, given the lower enterobactin concentration range used, similar or stronger
514 effects on the algae than those observed at high DFB could not be discarded.

515 **4.4 Stability of the apo- form versus the siderophore complex**

516 For enterobactin, the absence of the fragment 447 m/z or other metabolites is likely related to
517 the molecule's susceptibility to rapid degradation caused by hydrolysis of the ester linkages
518 present in the molecule (Leslie et al., 2007; Raymond et al., 1984). Winkelmann et al. (1994)
519 reported detection of the apo-form as well as FeEnterobactin degradation products by
520 *Escherichia coli* into mono-, di- and linear trimers after complex uptake and subsequent Fe
521 removal. However, some monomers seem to be produced very early (~28 h) and then
522 suddenly disappear from the medium. Despite the semi-continuous supply of the apo-
523 siderophore, the ~48 h gap between additions likely affected the detection time window due
524 to the rapid metabolization of the different metabolites. Another factor affecting
525 FeEnterobactin LC-MS detection is its tendency to dissociate. Although catechol
526 siderophores are characterized by extremely high-stability constants for Fe (Raymond et al.,
527 1984), the Fe exchange rate between competing ligands is not necessarily dictated by their
528 respective stability constants (Albrecht-Gary et al., 1998). Such is the case for enterobactin
529 which regardless the molecule's structure the complex exhibits a high dissociation rate
530 (Witter et al., 2000). It was therefore expected that enterobactin would facilitate diatom Fe
531 uptake by quick equilibration with FeEDTA and by serving as a Fe complexing shuttle
532 (Kustka et al., 2015). Despite Fe uptake rates were proportional to the enterobactin
533 concertation, only at the lowest treatment (0.01 nM: rate supply of 2 pM Fe-complex per
534 addition), the enhanced FSU and photosynthetic activity compared to Control, provided
535 support of potential benefits for *S. costaum* by facilitated Fe uptake.

In the case of DFB, the formation of the Fe-siderophore complex confers a remarkable chemical stability (Powell et al., 1983), which results in the formation of photostable complexes (Albrecht-Gary et al., 1998; Barbeau et al., 2003; Finden et al., 1984). The relative higher abundances of FeDFB in 10 nM and 500 nM DFB treatments contrasted with those in the 10,000 nM and the No-Algae 500 nM treatments. It could be possible that the FeDFB complex relative abundances could be the result of experimental artifact as changes in the speciation could have occurred during HPLC product of metals present in the system (Boiteau et al., 2013; Mawji et al., 2008; McCormack et al., 2003). Nevertheless, we draw attention to the relative abundances of DFB and FeDFB in each treatment. Furthermore, comparing the 10,000 nM DFB and the No-Algae 500 nM DFB treatments, the similar abundance profiles (despite one order of magnitude difference in addition) of the apo-siderophore argue for a decrease in the concentration in the former while its concentration remained relatively unaffected in the latter. This could be the result of possible siderophore degradation occurring in the 10,000 nM DFB. This is also supported by other studies which demonstrated that the apo-form of the siderophore is not photochemically reactive in natural sunlight (Barbeau et al., 2003).

4.5 Uptake of Fe-siderophore complex by the bacterial community

Final bacterial community abundance in all treatments showed no enhanced bacterial growth under either of the siderophore conditions. Since Fe uptake in the Control (EDTA-buffered) is assumed to be restricted to the dissociated Fe′ (Granger and Price, 1999), it can be argued that the heterotrophic bacteria associated to *S. costatum* was not able to uptake the entire FeDFB complex. The overall higher (up to 4-fold) Fe uptake in the presence of enterobactin compared to DFB at comparable concentrations is similar to responses reported with hydroxamate and catechol siderophores in isolated bacteria (Granger and Price, 1999). Nevertheless, uptake rates under both siderophores measured in this study were on average two orders of magnitude lower compared to Granger and Price (1999), who reported increased uptakes on Aquil + DFB for different bacterial strains. The fact that it was the Fe uptake in the associated bacteria and not in the isolated strains assessed in this study might partially account for the differences observed. The results of the uptake rates corresponded with an increase in the Fe:C ratio for all enterobactin treatments and at 10,000 nM DFB. This positive response was positively correlated to the increase in enterobactin concentrations, whereas the only significantly higher uptake in DFB occurred at 10,000 nM DFB when diatom exponential growth started at day 9. Yet this increase in Fe:C did not result in higher

bacterial abundances in any of the treatments with siderophore addition. While some studies revealed increases in bacterial abundance with Fe availability (Hutchins et al., 2001; Pakulski et al., 1996), others found no positive response to Fe alone but did see an increase in growth rate with the addition of both dissolved organic carbon (DOC) and Fe (Church et al., 2000). It could be argued that the bacteria were able to accumulate Fe but a lack of diatom growth may have not provided enough DOC for bacterial growth.

4.6 Siderophore bacterial degradation and potential role for *S. costatum* Fe uptake

The abundance profile at 10,000 nM DFB, comparable to that in the No-Algae 500 nM DFB likely reflected the molecule degradation in the former. Likewise, low abundances detected of siderophore metabolites in the No-Algae 500 nM DFB treatment suggests that the medium did not remain sterile, and that possible degradation occurred by bacteria remaining in the seawater after conditioning. Nonetheless, the 500 nM and the No-Algae 500 nM treatments despite having the same number of partial DFB additions over time, the relative abundances of the fragments 419.2503 m/z and 201.1240 m/z presented significant differences. This argues that the magnitude of the process occurring in the No-Algae treatment was not significant compared to that of the effect of the associated bacteria in the 500 nM treatment.

As Fe siderophore bound uptake in marine prokaryotes and eukaryotes can occur mediated by a cell-surface Fe(III) transporter or via extracellular reduction, in the latter bacteria can catabolize siderophores concomitant with their growth, with degradation patterns depending on bacterial strain and siderophore type (Pierwola et al., 2004 and cities therein). Thus the presence of either the entire apo-siderophore or its metabolites will depend on the way the complex is incorporated and metabolized. The degradation of DFB into a sequence of dihydroxamates and monohydroxamates has been previously reported (Castignetti and Siddiqui, 1990; Winkelmann et al., 1996), and corresponded with some of the compounds detected here thus supporting the argument of bacterial degradation of the apo-siderophore. However, the observed increase in the Fe to carbon ratio contrasts with the reduced bacterial growth observed, and raises the question of whether the bacteria associated with *S. costatum* were able to readily utilize any of the siderophore complexes. It could be speculated that the associated bacteria at the highest DFB concentrations were able to obtain both Fe and organic carbon by degrading the apo-siderophore in order to compensate for lack of algal biomass as a source. Although the apo-siderophore desferrioxamine represents a very uncommon C- and N-source, its simultaneous function as an Fe donor and as a carbon source cannot be excluded

(Winkelmann et al., 1999), as cases for this has been found in some terrestrial bacteria capable of growing on DFB as the sole carbon source (Castignetti and Siddiqui, 1990).

The Fe uptake rates reported here for *S. costatum* although comparable with Fe limited diatoms species such as from the genus Thalassiosira (Maldonado and Price, 2001; Shaked et al., 2005), at the highest DFB treatments reported uptake rates could not be accounted solely on the reductive mechanism. Alternatively, other mechanisms that could be proposed to account for the high Fe uptake at high DFB, could be a non-reductive pathway as recently proposed for certain *P. tricornutum*. Yet the genes likely be involved in the up-regulation for the "iron starvation induced proteins" (ISIPs) that could be involved in siderophore uptake, has not been found in *S. costatum* (Kazamia et al., 2018). The degradation of the excess DFB to alleviate a carbon deficiency by the associated bacteria, could have therefore altered the ligand concentration over time. Such changes would have likely favored the diatom Fe uptake, as less DFB would compete for Fe(III) with the Fe reduction mechanism at the diatom's surface. However a plausible alternative, this would need further research.

CONCLUSIONS

The overall physiological response of *S. costatum* at equivalent concentrations was different between the two siderophores. Enterobactin generated mixed responses depending of the variable measured, while it exhibit a more negative effect than DFB in traits such as fluorescence. On the other hand DFB at the highest concentrations exhibited more negative effects on the diatom's physiology in traits such as the FeQ. The overall siderophore effect on Fe bioavailability and uptake for *S. costatum* differed in the presence of cathecolate and hydroxamate siderophores.

The overall increase in Fe uptake observed in bacteria together with the negative correlation of the bacterial abundance over time with the concentration of both siderophores, constitutes evidence that bacteria associated with the diatom *S. costatum* were unable to readily utilize the Fe acquired. This highlights the link between the diatom and the associated bacteria based on the factors that were likely constraining the growth of both organisms. The capacity of the algae for acquiring Fe after a prolonged time at high DFB concentrations suggests that of changes in the concentration of the apo-siderophore, which is supported by the presence of DFB of the degradation metabolites revealed in the LC-MS analysis. It can only be speculated of the possibility for the bacteria to obtain carbon from the apo- form of the siderophore, thus reducing its concentration and shifting the Fe-ligand equilibrium with an

ultimate benefit for the Fe-membrane cell reduction by *S. costatum*. The combined results highlight the need to study the Fe bioavailability in interaction with other microbial components such as bacteria and over a time frame that reflects the natural ecosystem dynamics.

ACKNOWLEDGMENTS

We would like to thank to Kåre Andre Kristiansen, from the department of Biotechnology and Food Science at NTNU, with LC-MS analysis and Syverin Lierhagen for the ICP-MS analysis, at the Chemistry department at NTNU. To Andrew King and Keshuai Li for help with the protocols and analysis of Fe isotopes. We also thank the reviewers for the suggestions to improve this manuscript.

CONTRIBUTORS

Experimental design was conceived by MA and NS. CP and NS carried out the experiment and part of the analysis. Flow Cytometry and LC-MS analysis, where performed by OV and SG respectively. Writing was performed by NS with comments and discussion of the results with all others authors.

FUNDING

This work was supported by the Department of Chemistry, Faculty of Natural Sciences, Norwegian University of Science and Technology (NTNU). Additional support also provided by the EU project: Ocean Food-web Patrol–Climate Effects: Reducing Targeted Uncertainties with an Interactive Network. European Commission (OCEAN-CERTAIN, FP7-ENV-2013-6.1-1: no.: 603773).

REFERENCES

Albrecht-Gary, A., Crumbliss, A., Sigel, A. and Sigel, H., 1998. Metal ions in biological systems. A. SigelH. Sigel, ed., Marcel Dekker: New York, 35: 239-327.

Amin, S.A. et al., 2009. Photolysis of iron-siderophore chelates promotes bacterial-algal mutualism. Proc Natl Acad Sci U S A, 106(40): 17071-6.

Ardelan, M. et al., 2010. Natural iron enrichment around the Antarctic Peninsula in the Southern Ocean. Biogeosciences, 7(1): 11-25.

Baffi, F. and Cardinale, A., 1990. Improvements in use of Chelex-100 resin for determination of copper, cadmium and iron in sea water. International Journal of Environmental Analytical Chemistry, 41(1-2): 15-20.

Barbeau, K., Kujawinski, E. and Moffett, J., 2001. Remineralization and recycling of iron, thorium and organic carbon by heterotrophic marine protists in culture. Aquatic Microbial Ecology, 24(1): 69-81.

667 Barbeau, K., Rue, E.L., Trick, C.G., Bruland, K.W. and Butler, A., 2003. Photochemical reactivity of
668 siderophores produced by marine heterotrophic bacteria and cyanobacteria based on
669 characteristic Fe (III) binding groups. Limnology and Oceanography, 48(3): 1069-1078.
670 Berner, I., Greiner, M., Metzger, J., Jung, G. and Winkelmann, G., 1991. Identification of enterobactin
671 and linear dihydroxybenzoylserine compounds by HPLC and ion spray mass spectrometry
672 (LC/MS and MS/MS). Biology of metals, 4(2): 113-118.
673 Boiteau, R.M., Fitzsimmons, J.N., Repeta, D.J. and Boyle, E.A., 2013. Detection of iron ligands in
674 seawater and marine cyanobacteria cultures by high-performance liquid chromatography-
675 inductively coupled plasma-mass spectrometry. Anal Chem, 85(9): 4357-62.
676 Boiteau, R.M. et al., 2016. Siderophore-based microbial adaptations to iron scarcity across the
677 eastern Pacific Ocean. Proceedings of the National Academy of Sciences, 113(50): 14237-
678 14242.
679 Boukhalfa, H. and Crumbliss, A.L., 2002. Chemical aspects of siderophore mediated iron transport.
680 Biometals, 15(4): 325-339.
681 Braun, V., Hantke, K. and Koester, W., 1998. Bacterial iron transport: mechanisms, genetics, and
682 regulation. Metal ions in biological systems, 35: 67-146.
683 Breitbarth, E. et al., 2010. Iron biogeochemistry across marine systems–progress from the past
684 decade. Biogeosciences, 7(3): 1075-1097.
685 Bruland, K.W., Rue, E.L. and Smith, G.J., 2001. Iron and macronutrients in California coastal upwelling
686 regimes: Implications for diatom blooms. Limnology and Oceanography, 46(7): 1661-1674.
687 Butler, A. and Theisen, R.M., 2010. Iron (III)–siderophore coordination chemistry: reactivity of
688 marine siderophores. Coordination chemistry reviews, 254(3): 288-296.
689 Castignetti, D. and Siddiqui, A.S., 1990. The catabolism and heterotrophic nitrification of the
690 siderophore deferrioxamine B. Biology of metals, 3(3-4): 197-203.
691 Church, M.J., Hutchins, D.A. and Ducklow, H.W., 2000. Limitation of bacterial growth by dissolved
692 organic matter and iron in the Southern Ocean. Applied and Environmental Microbiology,
693 66(2): 455-466.
694 Dittmar, T., Koch, B., Hertkorn, N. and Kattner, G., 2008. A simple and efficient method for the solid-
695 phase extraction of dissolved organic matter (SPE-DOM) from seawater. Limnol. Oceanogr.
696 Methods, 6(6): 230-235.
697 Eldridge, M.L., Cadotte, M.W., Rozmus, A.E. and Wilhelm, S.W., 2007. The response of bacterial
698 groups to changes in available iron in the Eastern subtropical Pacific Ocean. Journal of
699 experimental marine biology and ecology, 348(1): 11-22.
700 Eldridge, M.L. et al., 2004. Phytoplankton community response to a manipulation of bioavailable iron
701 in HNLC waters of the subtropical Pacific Ocean. Aquatic Microbial Ecology, 35(1): 79-91.
702 Finden, D., Tipping, E., Jaworski, G. and Reynolds, C., 1984. Light-induced reduction of natural iron
703 (III) oxide and its relevance to phytoplankton. Nature, 309: 783-784.
704 Fukuda, R., Ogawa, H., Nagata, T. and Koike, I., 1998. Direct determination of carbon and nitrogen
705 contents of natural bacterial assemblages in marine environments. Applied and
706 environmental microbiology, 64(9): 3352-3358.
707 Gledhill, M., 2001. Electrospray ionisation-mass spectrometry of hydroxamate siderophores. Analyst,
708 126(8): 1359-1362.
709 Gledhill, M. and Buck, K.N., 2012. The organic complexation of iron in the marine environment: a
710 review. Front Microbiol, 3: 69.
711 Gledhill, M. et al., 2004. Production of siderophore type chelates by mixed bacterioplankton
712 populations in nutrient enriched seawater incubations. Marine Chemistry, 88(1): 75-83.
713 Gledhill, M. and van den Berg, C.M., 1994. Determination of complexation of iron (III) with natural
714 organic complexing ligands in seawater using cathodic stripping voltammetry. Marine
715 Chemistry, 47(1): 41-54.
716 Granger, J. and Price, N.M., 1999. The importance of siderophores in iron nutrition of heterotrophic
717 marine bacteria. Limnology and Oceanography, 44(3): 541-555.

718 Groenewold, G.S. et al., 2004. Collision-induced dissociation tandem mass spectrometry of
719 desferrioxamine siderophore complexes from electrospray ionization of UO22+, Fe3+ and
720 Ca2+ solutions. Journal of mass spectrometry, 39(7): 752-761.
721 Guillard, R.R., 1973. Division rates. Handbook of phycological methods, 1: 289-312.
722 Guillard, R.R. and Ryther, J.H., 1962. Studies of marine planktonic diatoms: I. Cyclotella Nana
723 Hustedt, and Detonula Confervacea (CLEVE) Gran. Canadian journal of microbiology, 8(2):
724 229-239.
725 Hassler, C. and Schoemann, V., 2009. Bioavailability of organically bound Fe to model phytoplankton
726 of the Southern Ocean. Biogeosciences, 6(10): 2281-2296.
727 Hassler, C.S., Schoemann, V., Nichols, C.M., Butler, E.C. and Boyd, P.W., 2011. Saccharides enhance
728 iron bioavailability to Southern Ocean phytoplankton. Proceedings of the National Academy
729 of Sciences, 108(3): 1076-1081.
730 Haygood, M.G., Holt, P.D. and Butler, A., 1993. Aerobactin production by a planktonic marine Vibrio
731 sp. Limnology and Oceanography, 38(5): 1091-1097.
732 Hopkinson, B.M. and Morel, F.M., 2009. The role of siderophores in iron acquisition by
733 photosynthetic marine microorganisms. Biometals, 22(4): 659-69.
734 Hudson, R.J., Covault, D.T. and Morel, F.M., 1992. Investigations of iron coordination and redox
735 reactions in seawater using 59Fe radiometry and ion-pair solvent extraction of amphiphilic
736 iron complexes. Marine Chemistry, 38(3-4): 209-235.
737 Hudson, R.J. and Morel, F.M., 1990. Iron transport in marine phytoplankton: Kinetics of cellular and
738 medium coordination reactions. Limnology and Oceanography: 1002-1020.
739 Hutchins, D., DiTullio, G., Zhang, Y. and Bruland, K., 1998. An iron limitation mosaic in the California
740 upwelling regime. Limnology and Oceanography, 43(6): 1037-1054.
741 Hutchins, D., Franck, V., Brzezinski, M. and Bruland, K., 1999a. Inducing phytoplankton iron limitation
742 in iron-replete coastal waters with a strong chelating ligand. Limnology and Oceanography,
743 44(4): 1009-1018.
744 Hutchins, D. et al., 2001. Control of phytoplankton growth by iron and silicic acid availability in the
745 subantarctic Southern Ocean: Experimental results from the SAZ Project. Journal of
746 Geophysical Research: Oceans, 106(C12): 31559-31572.
747 Hutchins, D.A., Witter, A.E., Butler, A. and Luther, G.W., 1999b. Competition among marine
748 phytoplankton for different chelated iron species. Nature, 400(6747): 858-861.
749 Johnson, K.S., Gordon, R.M. and Coale, K.H., 1997. What controls dissolved iron concentrations in
750 the world ocean? Marine Chemistry, 57(3–4): 137-161.
751 Kazamia, E. et al., 2018. Endocytosis-mediated siderophore uptake as a strategy for Fe acquisition in
752 diatoms. 4(5): eaar4536.
753 Kustka, A.B., Jones, B.M., Hatta, M., Field, M.P. and Milligan, A.J., 2015. The influence of iron and
754 siderophores on eukaryotic phytoplankton growth rates and community composition in the
755 Ross Sea. Marine Chemistry, 173: 195-207.
756 Kustka, A.B., Shaked, Y., Milligan, A.J., King, D.W. and Morel, F.M., 2005. Extracellular production of
757 superoxide by marine diatoms: Contrasting effects on iron redox chemistry and
758 bioavailability. Limnology and Oceanography: 1172-1180.
759 Laglera, L.M. and van den Berg, C.M., 2009. Evidence for geochemical control of iron by humic
760 substances in seawater. Limnology and Oceanography, 54(2): 610-619.
761 Leslie, A.D., Daneshfar, R. and Volmer, D.A., 2007. Infrared multiphoton dissociation of the
762 siderophore enterobactin and its Fe(III) complex. Influence of Fe(III) binding on dissociation
763 kinetics and relative energetics. J Am Soc Mass Spectrom, 18(4): 632-41.
764 Lis, H., Shaked, Y., Kranzler, C., Keren, N. and Morel, F.M., 2015. Iron bioavailability to
765 phytoplankton: an empirical approach. The ISME journal, 9(4): 1003-1013.
766 Maldonado, M.T. et al., 2001. Iron uptake and physiological response of phytoplankton during a
767 mesoscale Southern Ocean iron enrichment. Limnology and oceanography, 46(7): 1802-
768 1808.

Maldonado, M.T. and Price, N.M., 1999. Utilization of iron bound to strong organic ligands by plankton communities in the subarctic Pacific Ocean. Deep Sea Research Part II: Topical Studies in Oceanography, 46(11): 2447-2473.

Maldonado, M.T. and Price, N.M., 2001. Reduction and transport of organically bound iron by Thalassiosira oceanica (Bacillariophyceae). Journal of Phycology, 37(2): 298-310.

Maldonado, M.T., Price, N.M., PRICE, N. and PRICE, N., 2000. Nitrate regulation of Fe reduction and transport in Fe-limited Thalassiosira oceanica. Limnology and Oceanography, 45(4): 814-826.

Marie, D., Partensky, F., Jacquet, S. and Vaulot, D., 1997. Enumeration and cell cycle analysis of natural populations of marine picoplankton by flow cytometry using the nucleic acid stain SYBR Green I. Applied and Environmental Microbiology, 63(1): 186-193.

Martinez, J., Haygood, M. and Butler, A., 2001. Identification of a natural desferrioxamine siderophore produced by a marine bacterium. Limnology and Oceanography, 46(2): 420-424.

Mawji, E. et al., 2008. Hydroxamate Siderophores: Occurrence and Importance in the Atlantic Ocean. Environmental Science & Technology, 42(23): 8675-8680.

McCormack, P., Worsfold, P.J. and Gledhill, M., 2003. Separation and detection of siderophores produced by marine bacterioplankton using high-performance liquid chromatography with electrospray ionization mass spectrometry. Analytical chemistry, 75(11): 2647-2652.

McKay, R. et al., 2005. Impact of phytoplankton on the biogeochemical cycling of iron in subantarctic waters southeast of New Zealand during FeCycle. Global biogeochemical cycles, 19(4).

Öztürk, M. and Bizsel, N., 2003. Iron speciation and biogeochemistry in different nearshore waters. Marine Chemistry, 83(3–4): 145-156.

Öztürk, M., Steinnes, E. and Sakshaug, E., 2002. Iron Speciation in the Trondheim Fjord from the Perspective of Iron Limitation for Phytoplankton. Estuarine, Coastal and Shelf Science, 55(2): 197-212.

Pakulski, J.D., Coffin, R.B., Kelley, C.A. and Holder, S.L., 1996. Iron stimulation of Antarctic bacteria. Nature, 383(6596): 133.

Pierwola, A., Krupinski, T., Zalupski, P., Chiarelli, M. and Castignetti, D., 2004. Degradation pathway and generation of monohydroxamic acids from the trihydroxamate siderophore deferrioxamine B. Applied and environmental microbiology, 70(2): 831-836.

Powell, P.E., Szaniszlo, P.J. and Reid, C.P., 1983. Confirmation of occurrence of hydroxamate siderophores in soil by a novel Escherichia coli bioassay. Applied and environmental microbiology, 46(5): 1080-1083.

Price, N.M. et al., 1989. Preparation and chemistry of the artificial algal culture medium Aquil. Biological Oceanography, 6(5-6): 443-461.

Raymond, K.N., Dertz, E.A. and Kim, S.S., 2003. Enterobactin: an archetype for microbial iron transport. Proceedings of the National Academy of Sciences, 100(7): 3584-3588.

Raymond, K.N., Müller, G. and Matzanke, B.F., 1984. Complexation of iron by siderophores a review of their solution and structural chemistry and biological function, Structural Chemistry. Springer, pp. 49-102.

Reid, R.T., Livet, D.H., Faulkner, D.J. and Butler, A., 1993. A siderophore from a marine bacterium with an exceptional ferric ion affinity constant.

Rue, E.L. and Bruland, K.W., 1995. Complexation of iron (III) by natural organic ligands in the Central North Pacific as determined by a new competitive ligand equilibration/adsorptive cathodic stripping voltammetric method. Marine Chemistry, 50(1): 117-138.

Sanchez et al., 2018. Effect of siderophore on iron availability in a diatom and a dinoflagellate species: contrasting response in associated bacteria. Frontiers in Marine Science, 5: 118.

Schmidt, M. and Hutchins, D., 1999. Size-fractionated biological iron and carbon uptake along a coastal to offshore transect in the NE Pacific. Deep Sea Research Part II: Topical Studies in Oceanography, 46(11): 2487-2503.

Shaked, Y., Kustka, A.B. and Morel, F.M., 2005. A general kinetic model for iron acquisition by eukaryotic phytoplankton. Limnology and Oceanography: 872-882.

Shaked, Y. and Lis, H., 2012. Disassembling iron availability to phytoplankton. Front Microbiol, 3: 123.
Soria-Dengg, S. and Horstmann, U., 1995. Ferrioxamines B and E as iron sources for the marine diatom Phaeodactylum tricornutum. Marine Ecology Progress Series, 127: 269-277.
Soria-Dengg, S., Reissbrodt, R. and Horstmann, U., 2001. Siderophores in marine coastal waters and their relevance for iron uptake by phytoplankton: experiments with the diatom Phaeodactylum tricornutum. Marine Ecology Progress Series, 220: 73-82.
Strzepek, R.F., Maldonado, M.T., Hunter, K.A., Frew, R.D. and Boyd, P.W., 2011. Adaptive strategies by Southern Ocean phytoplankton to lessen iron limitation: Uptake of organically complexed iron and reduced cellular iron requirements. Limnology and Oceanography, 56(6): 1983-2002.
Sun, J. and Liu, D., 2003. Geometric models for calculating cell biovolume and surface area for phytoplankton. Journal of plankton research, 25(11): 1331-1346.
Tang, D. and Morel, F.M.M., 2006. Distinguishing between cellular and Fe-oxide-associated trace elements in phytoplankton. Marine Chemistry, 98(1): 18-30.
Tovar-Sanchez, A. et al., 2003. A trace metal clean reagent to remove surface-bound iron from marine phytoplankton. Marine Chemistry, 82(1-2): 91-99.
Velasquez, I. et al., 2011. Detection of hydroxamate siderophores in coastal and Sub-Antarctic waters off the South Eastern Coast of New Zealand. Marine Chemistry, 126(1-4): 97-107.
Vraspir, J.M. and Butler, A., 2009. Chemistry of Marine Ligands and Siderophores, Annual Review of Marine Science. Annual Review of Marine Science. Annual Reviews, Palo Alto, pp. 43-63.
Wells, M.L., 1999. Manipulating iron availability in nearshore waters. Limnology and Oceanography, 44(4): 1002-1008.
Wells, M.L., Price, N.M. and Bruland, K.W., 1994. Iron limitation and the cyanobacterium Synechococcus in equatorial Pacific waters. Limnology and Oceanography, 39(6): 1481-1486.
Wilhelm, S.W. et al., 2013. Elemental quotas and physiology of a southwestern Pacific Ocean plankton community as a function of iron availability. Aquatic Microbial Ecology, 68(3): 185-194.
Winkelmann, G. et al., 1999. Degradation of desferrioxamines by Azospirillum irakense: Assignment of metabolites by HPLC/electrospray mass spectrometry. Biometals, 12(3): 255-264.
Winkelmann, G., Cansier, A., Beck, W. and Jung, G., 1994. HPLC separation of enterobactin and linear 2, 3-dihydroxybenzoylserine derivatives: a study on mutants ofEscherichia coli defective in regulation (fur), esterase (fes) and transport (fepA). Biometals, 7(2): 149-154.
Winkelmann, G., Schmidtkunz, K. and Rainey, F.A., 1996. Characterization of a novel Spirillum-like bacterium that degrades ferrioxamine-type siderophores. BioMetals, 9(1): 78-83.
Witter, A.E., Hutchins, D.A., Butler, A. and Luther, G.W., 2000. Determination of conditional stability constants and kinetic constants for strong model Fe-binding ligands in seawater. Marine Chemistry, 69(1): 1-17.

Figures and Tables

Table 1. Experimental setup with the diatom *Skeletonema costatum.* Background dissolved labile iron (DFe) concentration (nM). Iron + EDTA added in the medium (nM). Siderophore type and final concentrations (nM) after five additions. Rate DFB and Rate Ent: partial concentrations (nM) added every third day.

DFe (nM)	FeEDTA (nM)	DFB (nM)	Rate DFB (nM d^{-1})	[DFB]:[Fe]	Enterobactin (nM)	Rate Enterobactin (nM d^{-1})	[Ent]:[Fe]
1.22	40	**Control**			**Control**		
1.22	40	10	2	0.2	0.01	0.002	0.0002
1.22	40	50	10	1.2	0.05	0.01	0.001
1.22	40	500	100	12	0.5	0.1	0.012
1.22	40	2500	500	61	2.5	0.5	0.06
1.22	40	10000	2000	243	50	10	1.2

Table 2. Iron 55 uptake rate by Fe:C ratio (µmol mol h^{-1}; left), for *Skeletonema costatum* and bacterial community, by area (mol μm^2 h^{-1}; right) for *S. costatum* and by cell (mol cell h^{-1}; right) for the bacterial community measured at day 9 for each treatment with desferrioxamine (DFB) (nM) and enterobactin (nM). Standard deviation in parenthesis (n=3)

Siderophore	Treatment	*S. costatum* Fe:C (µmol h^{-1})		Bacteria Fe:C (µmol h^{-1})		*S. costatum* Fe (mol μm^2 h^{-1})		Bacteria Fe (mol Cell h^{-1})	
	Control	0.003	(0,001)	0.035	(0,002)	0,04 E-21	(0,003)	2.24E-22	(0.224)
DFB	**10**	0.007	(0,001)	0.013	(0,001)	0,07 E-21	(0,004)	0.88E-22	(0.123)
	500	0.018	(0,001)	0.015	(0,006)	0,08 E-21	(0,008)	0.59E-22	(0.070)
	10000	0.062	(0,018)	0.048	(0,002)	1,25 E-21	(0,137)	5.27E-22	(0.474)
Enterobactin	**0.01**	0.004	(0,001)	0.040	(0,014)	0,07 E-21	(0,002)	2.58E-22	(0.258)
	0.5	0.007	(0,005)	0.050	(0,011)	0,15 E-21	(0,018)	3.20E-22	(0.448)
	50	0.009	(0,005)	0.061	(0,016)	0,10 E-21	(0,005)	3.93E-22	(0.471)

Table 3. Parallel setup with the diatom *Skeletonema costatum* for the siderophore and dissolved organic matter analysis. No-Algae (500 and 0.5) corresponded to the same seawater medium with the addition of 500 and 0.5 nM for desferrioxamine B and enterobactin respectively. Siderophore additions followed same procedure as the main setup.

S. Costatum	**DFB (nM)**	No-Algae (500)	10	500	10000
	Enterobactin (nM)	No-Algae (0.5)	0.01	0.5	50

Table 4. Dissolved labile iron concentration (DFe) measured at the final day for each experiment performed with desferrioxamine (DFB) (nM) and enterobactin (nM). Value in parenthesis correspond to standard deviation (n = 3). n.d.: no data.

DFB		**10**	**50**	**500**	**2500**	**10000**
	Control	0.66 (0.3)	0.83 (0.2)	n.d.	1.26 (0.3)	1.59 (0.2)
Enterobactin	1.35 (0.1)	**0.01**	**0.05**	**0.5**	**2.5**	**50**
		n.d.	0.93 (0.2)	1.22 (0.1)	0.96 (0.3)	2.04 (0.2)

928 **Table 5.** Identification of siderophore, in the apo- form (uncomplexed) for desferrioxamine an enterobactin, the Fe-siderophore complex
929 (Ferrioxamine) and the tentative metabolites for desferrioxamine through HPLC-ESI-MS analysis. Fragment identification for DFB after collision
930 induced dissociation (CID).

931

932

933

Compound ion (m/z)	Ion Observed	Retention time (min)	Formula	ppm error	Fragment CID	Compound	Reference
561.3616	[M+H]	4.30	C25H48N6O8	1.76	443.2492 401.2395 319.2341	Desferrioxamine B	Velazquez et al., 2011
614.2710	[M+H]	2.95	C25H45N6O8Fe	-1.77		Ferrioxamine B	Velazquez et al., 2011
419.2503	[M+H]	3.41	C18H34N4O7	0.7		Dihydroxamete metabolite	Winkelmann et al., 1999
319.2348	[M+H]	4.26	C14H30N4O4	2.44		Monohydroxamate metabolite	Winkelmann et al., 1999
201.1240	[M+H]	4.31	C9H16N2O3	2.93		Monohydroxamate metabolite	Groenewold et al., 2004
670.1525	[M+H]	9.81	C30H27N3O15	1.5		Enterobactin	Berner et al., 1990

934

935

Figure 1. pH, In-Vivo fluorescence (FSU) and photosynthetic efficiency (Fv/Fm) for *S. costatum* cultures with desferrioxamine B (nM) (a, c, e and g) and enterobactin (b, d, f, and h) (nM) over time. Error bars: standard deviation (n=3).

Figure 2. Growth rate (Doublings d^{-1}) for *S. costatum* measured at exponential phase for each treatment with desferrioxamine B and enterobactin.

Figure 3. Particulate Iron (PFe) to particulate phosphorus ratio (PFe: PP), diatom Fe uptake ratio (Fe:C) (pmol µmol h^{-1}) for *S. costatum* with a) desferrioxamine B and b) enterobactin at day 9 and day 13 (final). Error bars: standard deviation (n=3).

Figure 4. Bacterial abundance (cell μL^{-1}) (a and b) in all treatments in *S. costatum* cultures with desferrioxamine B (nM) and enterobactin (nM). Error bars: standard deviation (n=3).

Figure 5. Particulate Iron (PFe) in the 0.2 µm fraction representing the bacterial community Fe uptake ratio (Fe:C) (µmol mol h^{-1}) in *S. costatum* cultures with a) desferrioxamine B and b) enterobactin at day 9. Error bars: standard deviation (n=3).

Figure 6. Standardized normalized abundance for a.) desferrioxamine B and b.) the Fe siderophore complex Ferrioxamine B in all the treatments at day 9 in the cultures with desferrioxamine B. The standard deviation corresponds to two samples and six subsamples per treatment.

Figure 7. PCA biplot for components 1 and 2 for the desferrioxamine B treatments: 10 nM (triangles), 500 nM (circles), 10,000 nM (squares) and No-Algae 500 nM (stars). Sample replicates are shown as symbols and desferrioxamine B (left) and ferrioxamine B (right) compounds are highlighted. All other compound ions are as grey numbers in the background.

Figure 8. Standardized normalized abundance for desferrioxamine B tentative metabolite, a.) the dihydroxamate 419.2503 eluted at 3.41, and b.) the monohydroxamates 319.2348 and c.) 201.1240 eluted at 4.26 and 4.31 min respectively. The distribution of points corresponds to two samples and six subsamples per treatment.

Figure 9. Standardized normalized abundance for enterobactin in all the treatments at day 9 in the cultures with enterobactin. The standard deviation corresponds to two samples and six subsamples per treatment.

Figure 10. PCA biplot for components 1 and 2 for the enterobactin treatments: 0.01 nM (triangles), 0.5 nM (circles), 50 nM (squares) and No-Algae (Control) 0.5 nM (stars). Sample replicates are shown as symbols and enterobactin compound is highlighted. All other compound ions are as grey numbers in the background.

Figure 1.

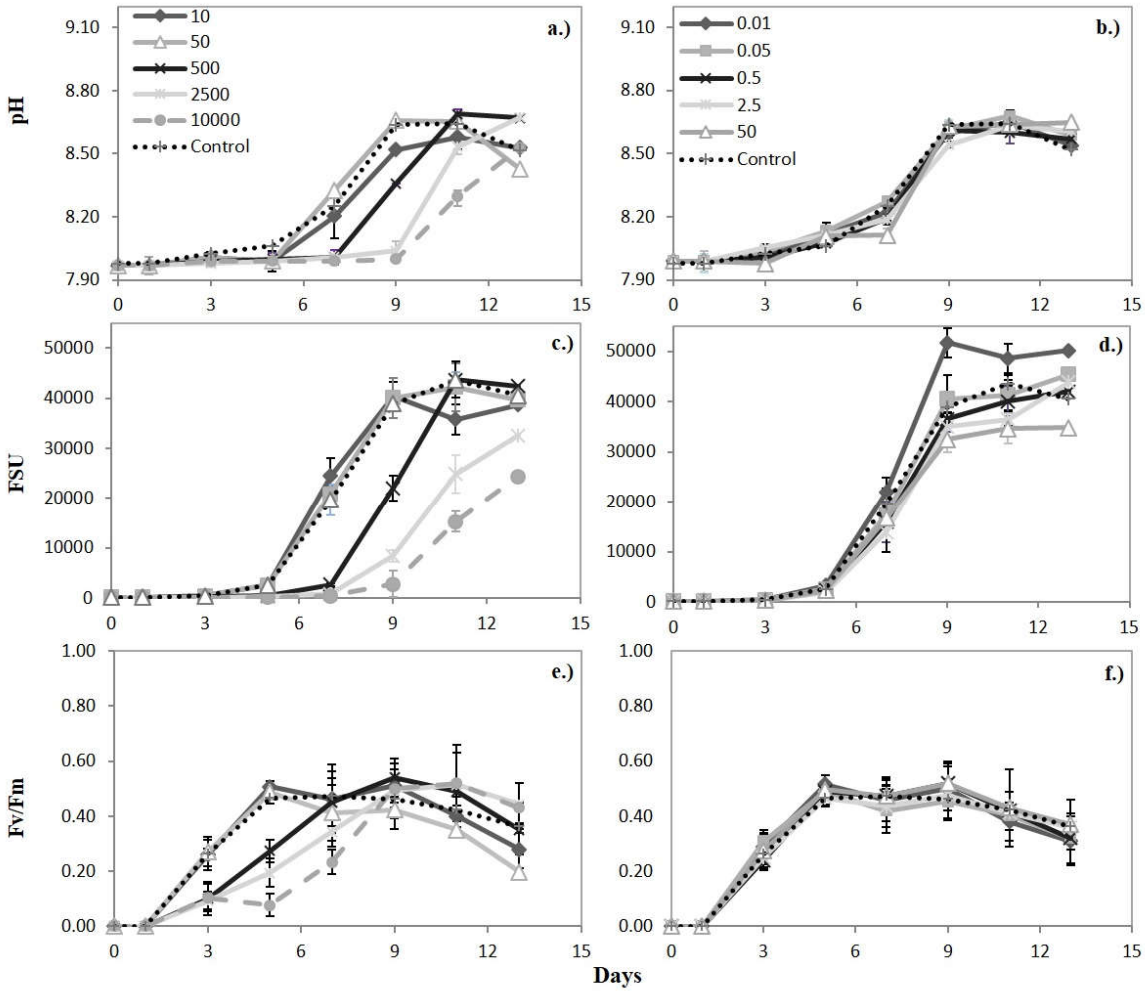
a.)
10
50
500
2500
10000
Control
pH
b.)
0.01
0.05
0.5
2.5
50
Control
c.)
FSU
d.)
e.)
Fv/Fm
f.)
Days

Figure 2.

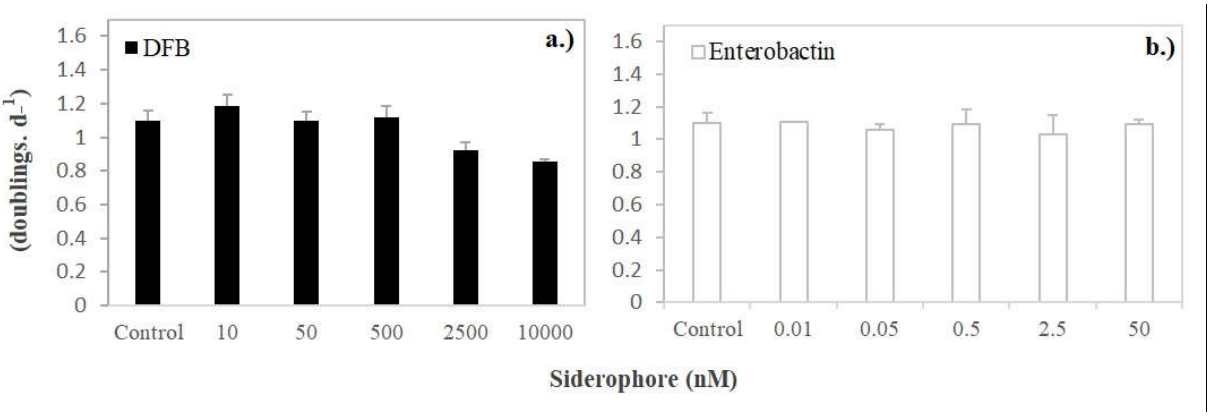
DFB
a.)
(doublings. d-1)
1.6
1.4
1.2
1
0.8
0.6
0.4
0.2
0
Control
10
50
500
2500
10000
Enterobactin
b.)
Control
0.01
0.05
0.5
2.5
50
Siderophore (nM)

Figure 3.

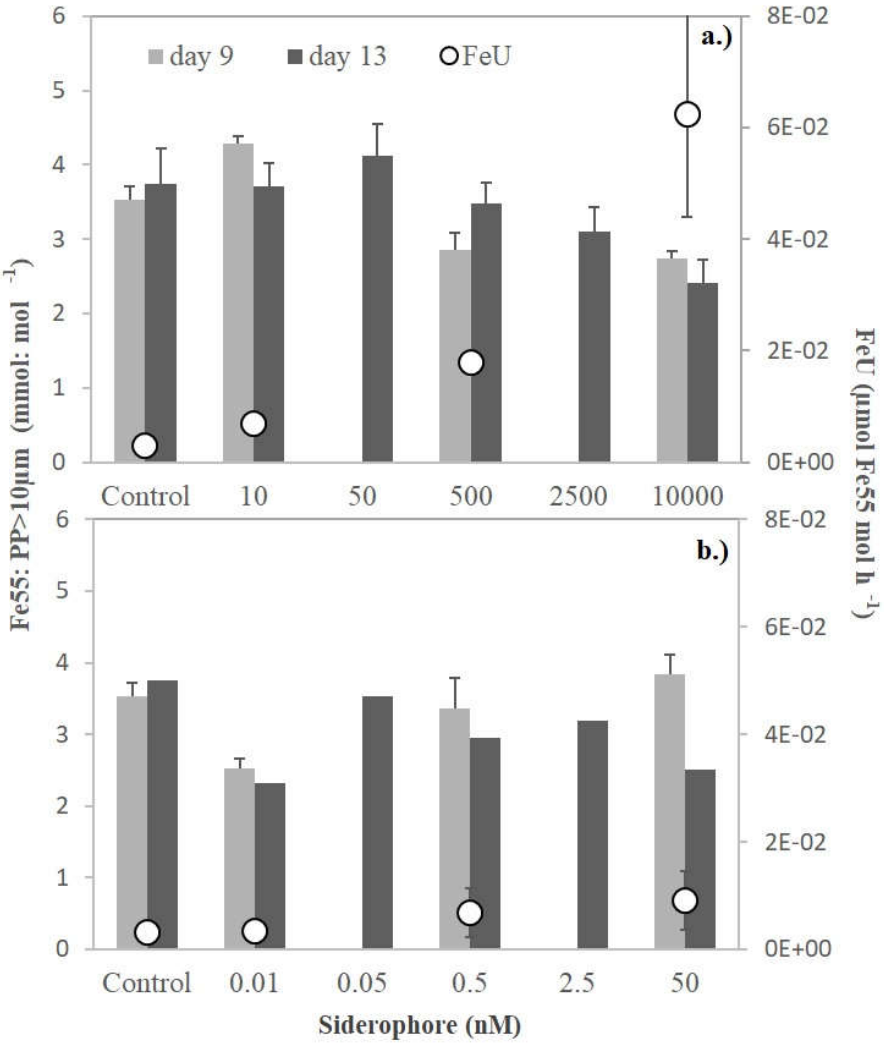
a.)
b.)
day 9
day 13
FeU
Fe55: PP>10µm (mmol: mol -1)
FeU (µmol Fe55 mol h -1)
Control
10
50
500
2500
10000
0.01
0.05
0.5
2.5
50
Siderophore (nM)

Figure 4.

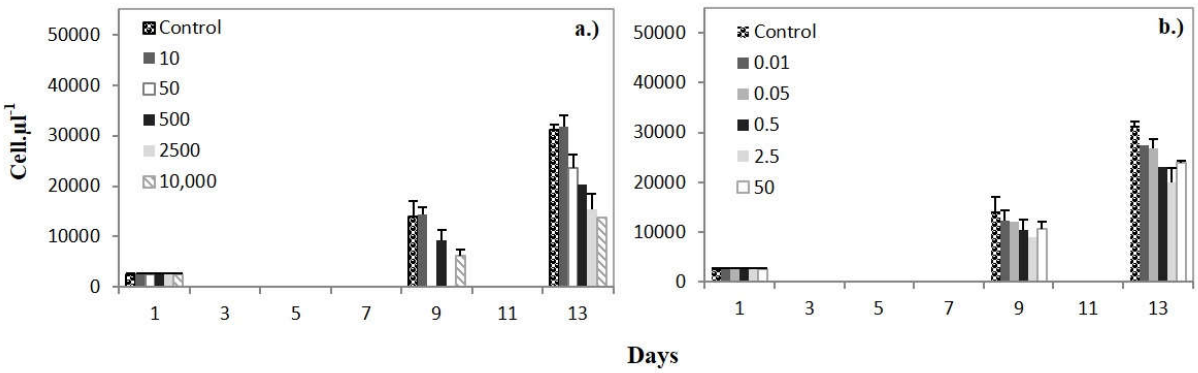
a.)
Control
10
50
500
2500
10,000
Cell.µl-1
50000
40000
30000
20000
10000
0
1
3
5
7
9
11
13
b.)
Control
0.01
0.05
0.5
2.5
50
Days

Figure 5.

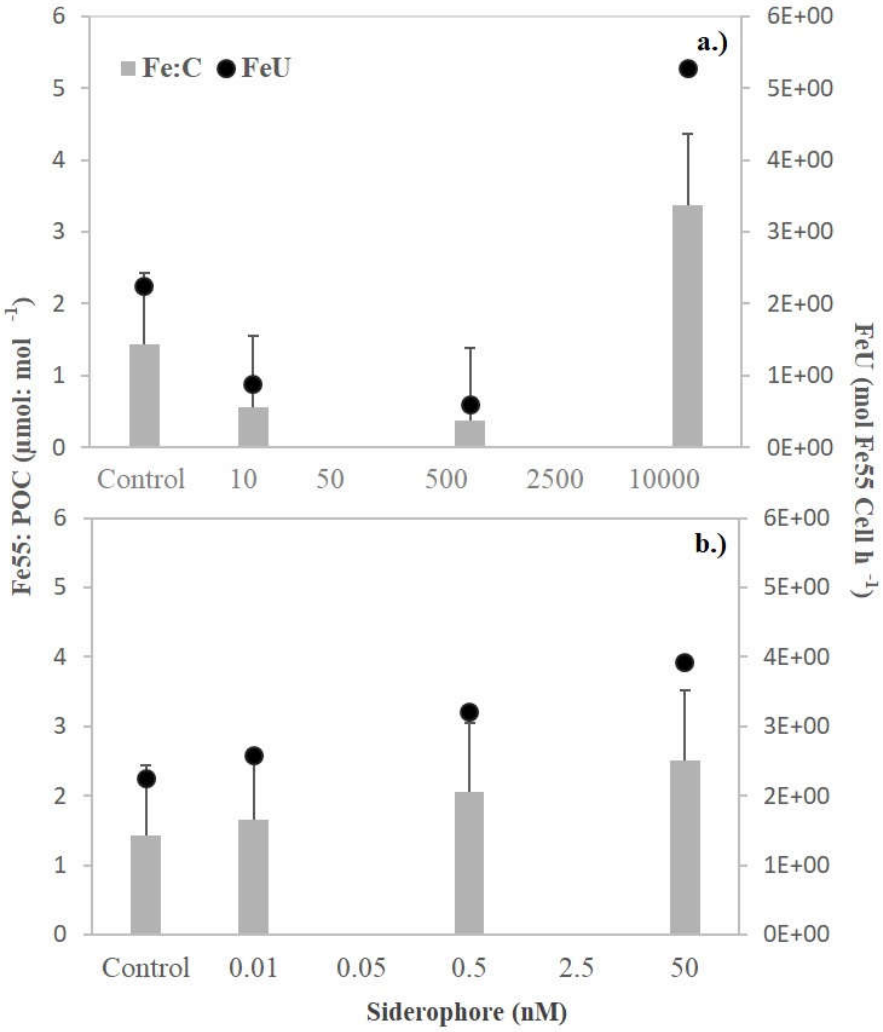
a.)
Fe:C
FeU
b.)
Fe55: POC (µmol: mol -1)
FeU (mol Fe55 Cell h -1)
Control
10
50
500
2500
10000
0.01
0.05
0.5
2.5
50
Siderophore (nM)

Figure 6.

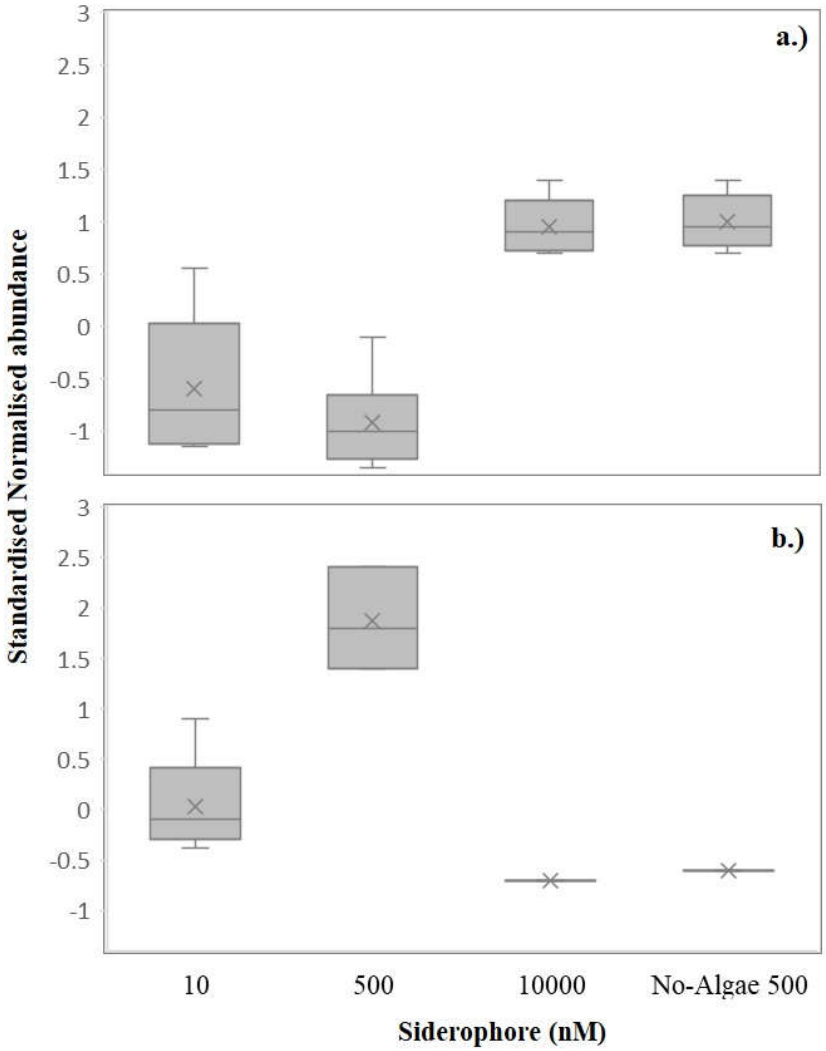
a.)
b.)
Standardised Normalised abundance
3
2.5
2
1.5
1
0.5
0
-0.5
-1
10
500
10000
No-Algae 500
Siderophore (nM)

Figure 7.

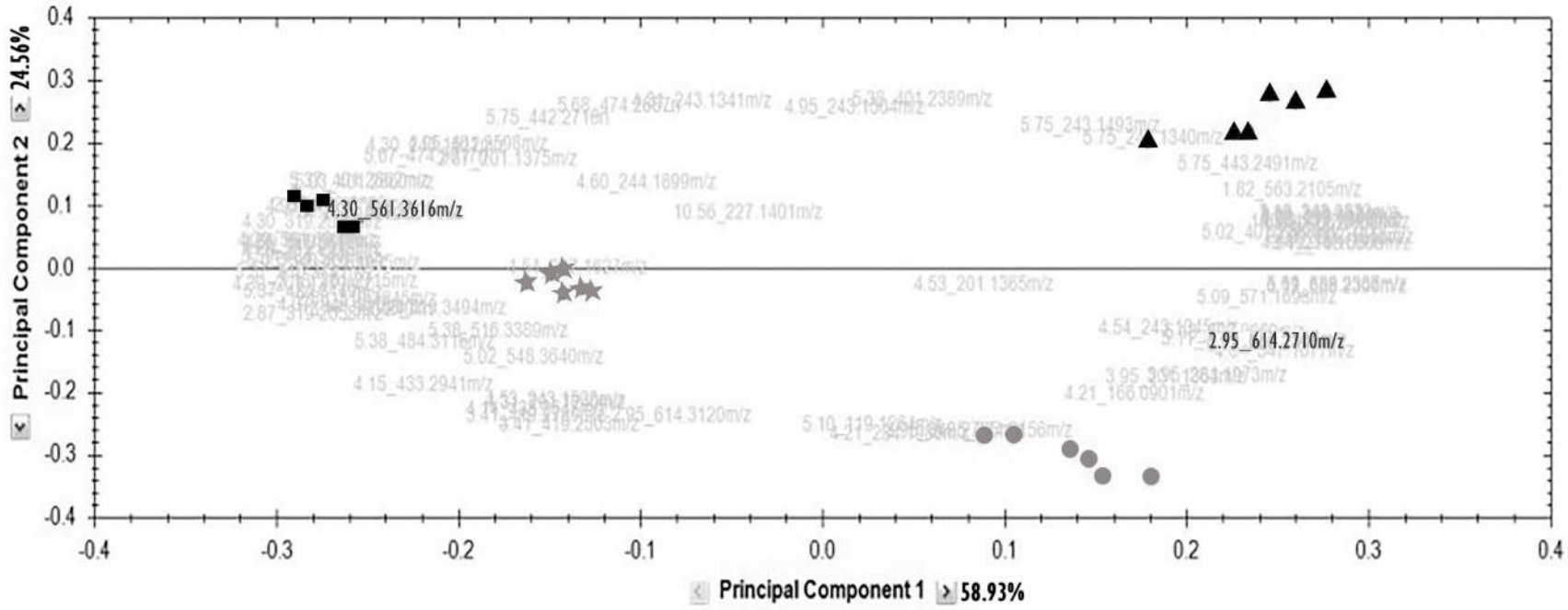
Principal Component 2 24.56%
Principal Component 1 58.93%
4.30_561.3616m/z
2.95_614.2710m/z
0.4
0.3
0.2
0.1
0.0
-0.1
-0.2
-0.3
-0.4
-0.4
-0.3
-0.2
-0.1
0.0
0.1
0.2
0.3
0.4

Figure 8.

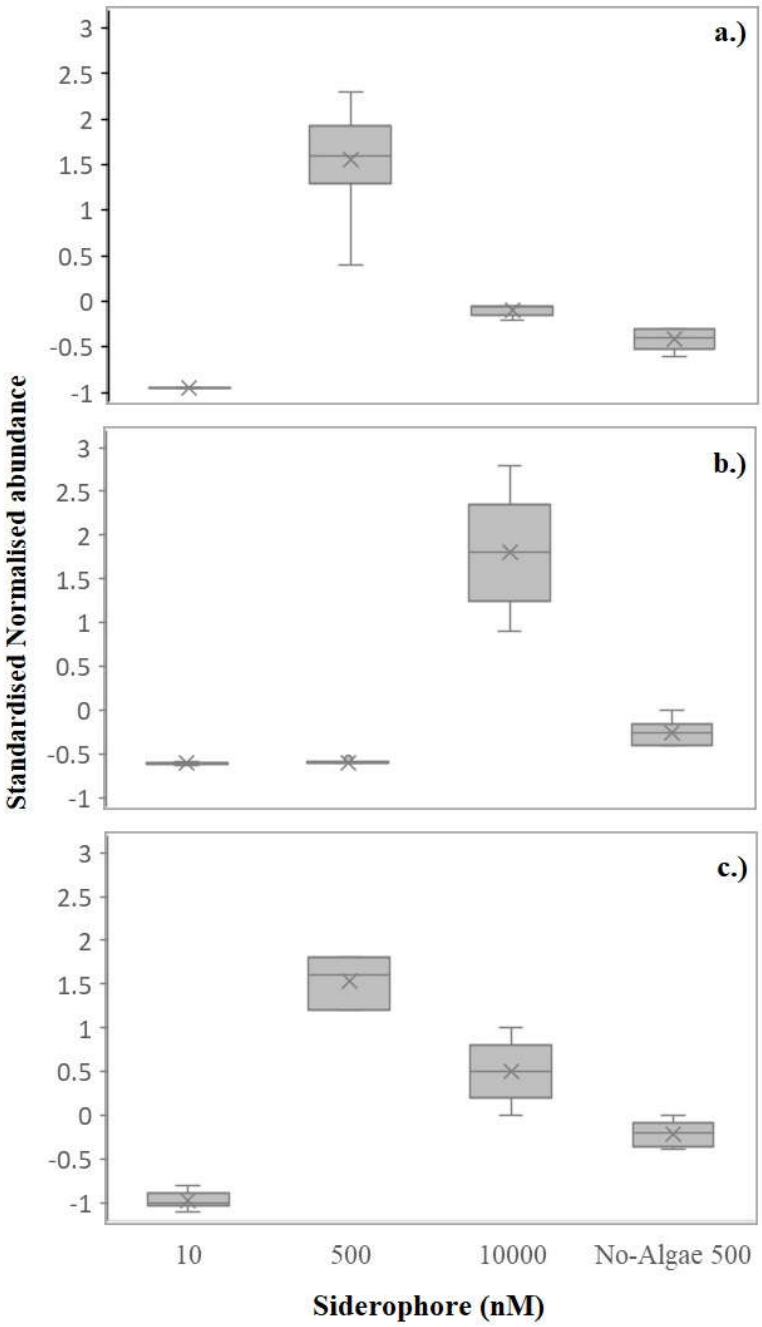
a.)
b.)
c.)
Standardised Normalised abundance
3
2.5
2
1.5
1
0.5
0
-0.5
-1
10
500
10000
No-Algae 500
Siderophore (nM)

Figure 9.

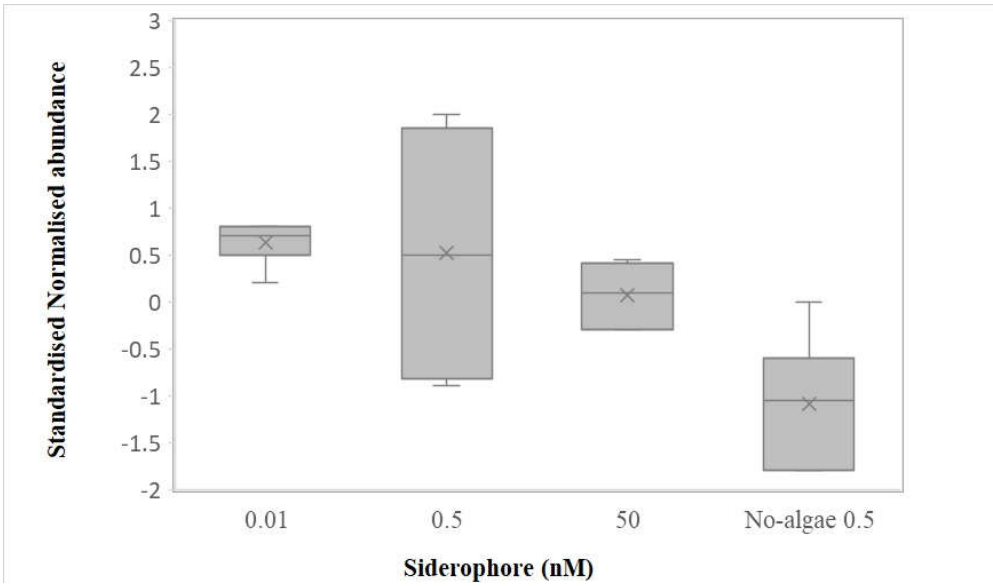
Standardised Normalised abundance
3
2.5
2
1.5
1
0.5
0
-0.5
-1
-1.5
-2
0.01
0.5
50
No-algae 0.5
Siderophore (nM)

Figure 10.

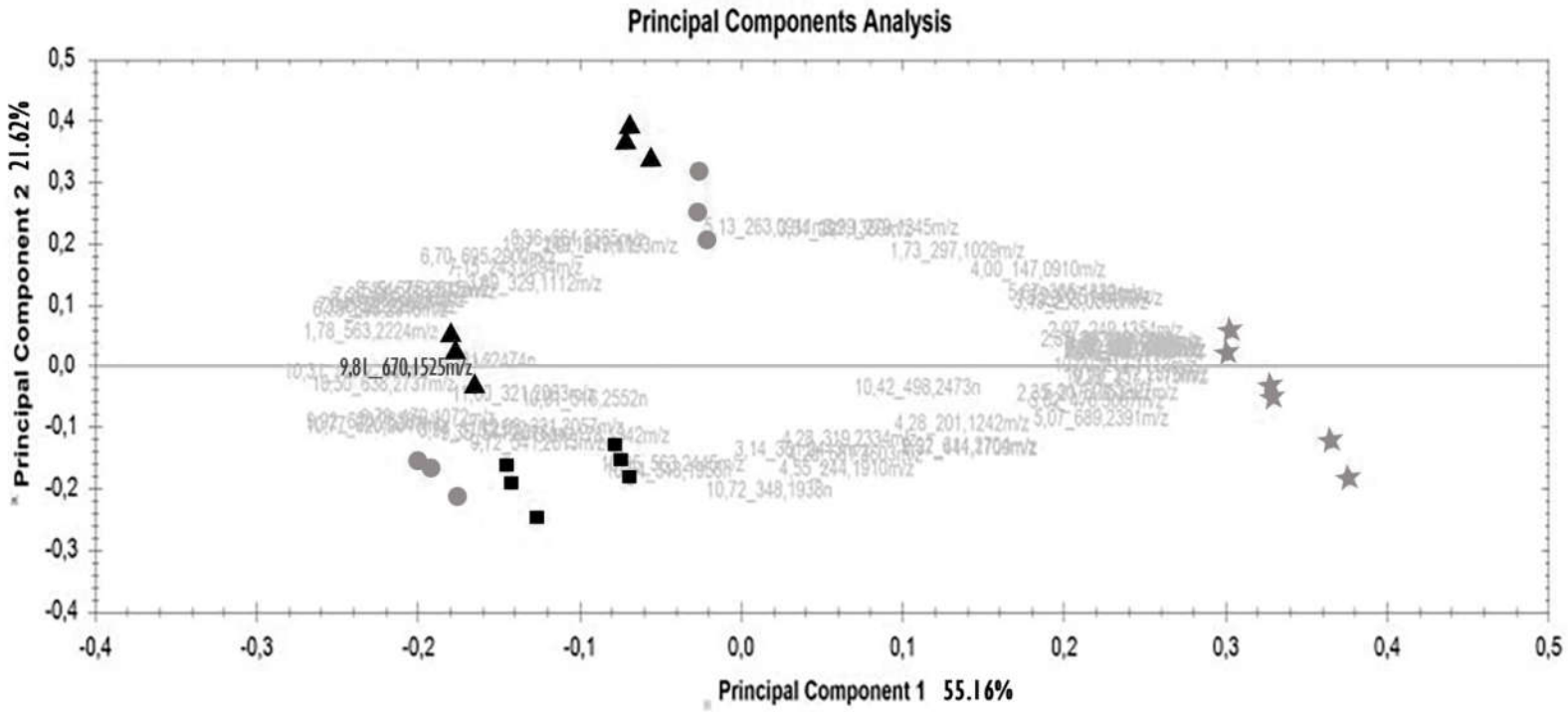
Principal Components Analysis
Principal Component 2 21.62%
Principal Component 1 55.16%
0,5
0,4
0,3
0,2
0,1
0,0
-0,1
-0,2
-0,3
-0,4
-0,4
-0,3
-0,2
-0,1
0,0
0,1
0,2
0,3
0,4
0,5
9,81_670,1525m/z
1,73_297,1029m/z
4,00_147,0910m/z
1,78_563,2224m/z
10,42_498,2473n
4,28_201,1242m/z
5,07_689,2391m/z
10,72_348,1938n